



EVALUATION OF CHLORIDE CONTENT IN CONCRETE BY X-RAY FLUORESCENCE

Edoardo Proverbio^{*} and Fabio Carassiti^{**}

^{*}University of Rome "La Sapienza", Dept. ICMMPM, Rome, Italy

^{**}Third University of Rome, Dept. of Mechanics and Automation, Rome, Italy

(Refereed)

(Received January 6, 1997; in final form June 10, 1997)

ABSTRACT

Determination of chloride content in concrete structures can be carried out by the X-ray fluorescence technique. However some problems affect measurement validity and limit the convenience of using XRF analysis when a limited number of determinations have to be performed. Measurements carried out on chloride contaminated concrete and mixtures of NaCl and concrete show the influence of distribution and grain size of chloride containing phase on analytical results. It is shown that chloride fluorescence intensity, at the same concentration level and at very low concentrations, is greatly reduced when chloride is present in the concrete matrix as NaCl salt instead of being dissolved in the concrete pore solution. © 1997 Elsevier Science Ltd

Introduction

In order to evaluate the initiation time to corrosion due to chloride in reinforced concrete structures, and to estimate the residual service life, it is necessary to know the chloride penetration depth as well as the chloride concentration profile.

Chloride content in concrete can be determined by means of a number of classical methods: argentometric titration, potentiometric measurements (ion selective electrodes) and atomic absorption (1). All of these methods, even if quite precise, require a long time to be carried out, and would take a lot of time during a measurement campaign on large structures.

Other techniques have been proposed to estimate chloride penetration resistance, such as the determination of the electrical conductance of concrete, (2) and the chloride penetration front by means of a colorimetric test (3), but in both the cases we cannot obtain a quantitative evaluation of chloride concentration, which is necessary to predict the corrosion probability of rebars (4,5,6).

A further analytical technique which can be used to determine chloride content in concrete structures is X-ray fluorescence (XRF) (7,8,9). When a great number of measurements have to be carried out XRF is a suitable analytical method allowing the analyzer to perform a greater number of determinations in a relatively short time compared to the other techniques.

A limited number of problems could however affect the measurement validity. The presence of humidity in measurement samples (pressed powder disks) can cause water migration toward the external surface when measurements are carried out in vacuum or in a dry atmos-

phere, thus causing an increase of chloride content on the sample surface and a consequent alteration of measurement results (8).

Element characteristic X-ray intensities emitted by the sample depend not only on element concentration but also on powder grain size, degree of compaction and the chemical bindings of the element in the matrix (8). Using fused samples to avoid the influence of sample heterogeneity can cause selective evaporation of some constituents (10). Preparation of samples and of calibration standards are of critical importance for the accurate evaluation of chloride content in concrete.

Usually standards are obtained starting from an uncontaminated concrete portion of the same type as that to be analyzed to which known amounts of chloride are added. Several measurements carried out by means of different analytical techniques have evidenced that XRF measurements obtained in such a way are affected by a systematic error, which disappears when, as calibration samples, chloride contaminated portions of concrete, whose chloride concentration were previously evaluated by chemical titration, are used.

In the present work, results of experimental research carried out to evaluate consistency of these errors and causes are reported.

Experimental

Sample Type. Two different experiments were carried out. A first measurement sequence was performed on chloride contaminated concrete samples (Sample C) obtained from large reinforced concrete slabs ($150 \times 70 \times 35$ cm) previously subject to periodical pouring with a sodium chloride solution to accelerate chloride ingress (11). Slabs were made using three 42.5 MPa strength class cements: one pozzolanic, one slag and one normal portland. Concrete mix design and the characteristics of each slab are summarized in Table 1. After two years of exposure 5 cm diameter cores were extracted from the contaminated surface. Chloride concentration was evaluated in 2 cm thick core sections. XRF calibration standards were obtained starting from uncontaminated concrete cored at a depth greater than 10 cm. To the ground concrete (see below) determined amounts of NaCl were added in order to obtain the following chloride concentrations (wt % by concrete): 0, 0.04, 0.08, 0.1, 0.3, 0.6, 1.0. XRF measurements were then compared to the results obtained by a standard analytical technique (Argentometric Titration).

To better understand the influence of morphology and composition of the chloride containing phase a second measurement campaign was carried out on three different sample series starting from the same pozzolanic concrete mixture (Table 2). Samples were cylinders 10 cm in diameter and 10 cm high. A first sample set was obtained by adding (sample A) NaCl to mixing water in concentrations ranging from 0 to 0.18 (wt% by concrete). The second set was obtained starting from the uncontaminated concrete mixture. After curing for 30 days the concrete was ground and subsequently mixed with ground NaCl to obtain four different chloride concentrations (wt% by concrete) between 0.08 and 0.6 (samples G). Further samples were also obtained by mixing NaCl ground for different times separately from the concrete. The last sample set consisted of four specimens into which, after curing (30 days), chloride was forced to penetrate into by means of an electromigration process (Sample E). A 50 V continuous tension was applied between a stainless steel net embedded at the bottom of the sample itself and a titanium net positioned above the upper sample surface and dipped in a NaCl saturated solution. Electromigration was allowed to continue for different times in order to obtain different chloride concentrations in the sample. At the

TABLE 1
Mix Design of C Type Concrete Specimens

Slab No.	Cement Strength class MPa	Cement designation	Cement factor kg/m ³	Aggregates kg/m ³	Mixture proportion	Coarse aggr. max size	Admixture	Dosage % c. + l/m ³	W/C	Air %
									s.s.d.	
4 PT	42.5	Portland I	350	1900	50% gravel	35 mm rounded	D.200	0.84 + 0	0.50	1.0
5 PT	42.5	Portland I	350	1900			D.200/DCI.S	0.80 + 10	0.50	0.7
6 PT	42.5	Portland I	350	1900			D.200/DCI.S	0.80 + 15	0.50	0.7
4 PZ	42.5	Pozzolanic II/B-S	350	1900	35% coarse sand		D.200	0.90 + 0	0.50	0.7
5 PZ	42.5	Pozzolanic II/B-S	350	1900			D.200/DCI.S	0.90 + 10	0.50	0.5
6 PZ	42.5	Pozzolanic II/B-S	350	1900			D.200/DCI.S	0.90 + 15	0.50	0.6
4 SC	42.5	Slag cement IV/A	350	1900	15% sand		D.200	0.70 + 0	0.50	0.4
5 SC	42.5	Slag cement IV/A	350	1900			D.200/DCI.S	0.70 + 10	0.50	0.5
6 SC	42.5	Slag cement IV/A	350	1900			D.200/DCI.S	0.70 + 15	0.50	0.4

Note: D.200 = superplasticizer (ASTM C494 Type F)
DCI.S= calcium nitrite corrosion inhibitor

TABLE 2
Mix Design of A, G and E Type Concrete Specimens

Cement Strength class	Cement designation	Cement factor kg/m ³	Aggregates kg/m ³	Mixture proportion	Coarse aggr. max size	W/C s.s.d.	Air %
MPa							
32.5	Pozzolanic II/B-S	350	1923	50% gravel 50% coarse sand	10 mm	0.50	2.0

end of the process, samples were cleaned in order to remove any salt deposit on the upper surface, then crushed, and only the first upper 5 centimetres were used to prepare samples for XRF measurements. In all the cases chloride content in the samples was evaluated by means of argentometric titration.

TABLE 3
Results of X-Ray Fluorescence and Chemical Analysis on C Type Samples
(wt.% by Concrete)

Cement type	Slab type	Sample depth (cm)	XRF	Argentometry
PT	4	0-2	1.19	0.24
		2-4	0.39	0.085
		>4	0.16	-
	5	0-2	0.85	0.19
		2-4	0.31	0.071
		>4	-	-
	6	0-2	1.33	0.32
		2-4	0.33	0.063
		>4	-	-
PZ	4	0-2	1.37	0.35
		2-4	0.24	0.034
		>4	-	-
	5	0-2	1.23	0.31
		2-4	0.20	0.051
		>4	0.09	-
	6	0-2	1.37	0.28
		2-4	0.26	0.057
		>4	-	0.01
SC	4	0-2	1.8	-
		2-4	0.1	0.04
		>4	0.04	0.027
	5	0-2	1.38	0.23
		2-4	0.08	0.028
		>4	-	-
	6	0-2	1.01	0.20
		2-4	0.04	0.019
		>4	-	-

Chloride Determination. The chloride content in all the samples was evaluated by chemical titration (1). Concrete was pulverized in a mortar, then a certain amount of powder dissolved in nitric acid. The solution obtained was then filtered and a known volume of this solution was titrated by a AgNO_3 solution.

XRF Measurements. The samples to be analyzed were crushed in a jaw crusher to obtain a grain dimension of about 2 mm. 20 g of crushed concrete was collected by quartering and dried at 105°C to reach a constant weight. Then a further grinding was performed by an eccentric mill for 60 s to obtain a powder finer than $180\ \mu\text{m}$. Before mill grinding, 10 wax pellets (0.8 g) were mixed with the concrete powder. Finally disks were made by pressing 11.5 g of powder at 300 MPa in an aluminium capsule.

XRF measurements were carried out by means of unfiltered Rh radiation (40 kV excitation voltage and 5 mA excitation current) in a He atmosphere (0.1 MPa). Counts were collected for 100s on the 2.622 KeV $\text{K}_{\alpha 1}$ chlorine peak by a WDS LiF 200 monochromator system.

Results

Chloride determination performed on the first sample type (C) by XRF, calculated by using uncontaminated concrete with added NaCl standards, are reported in Table 3. Measurements obtained by chemical titration are also reported. It is interesting to note that the XRF calculated chloride concentrations were much higher than the real ones (Figure 1). If such chloride concentrations are compared with those ones obtained by using as calibration standards contaminated concrete, whose chloride concentrations were previously evaluated by means of chemical titration (dashed line in Figure 1), such a difference is better evidenced.

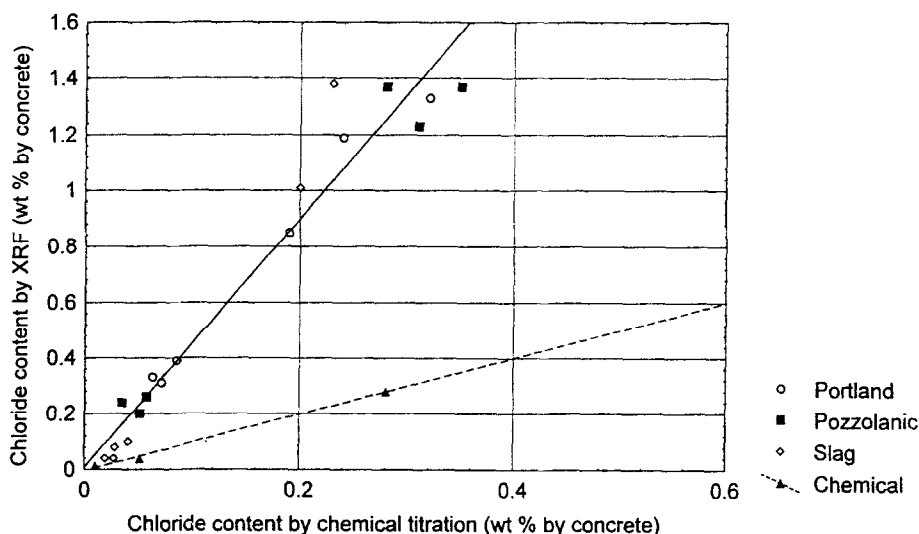


FIG. 1.

Chloride content in C type samples evaluated by XRF vs. effective chloride determined by chemical titration. \circ \blacksquare \diamond Measurements carried out by using NaCl-concrete mixtures as calibration standards; \blacktriangle Measurements carried out by using chloride contaminated concrete samples as calibration standards.

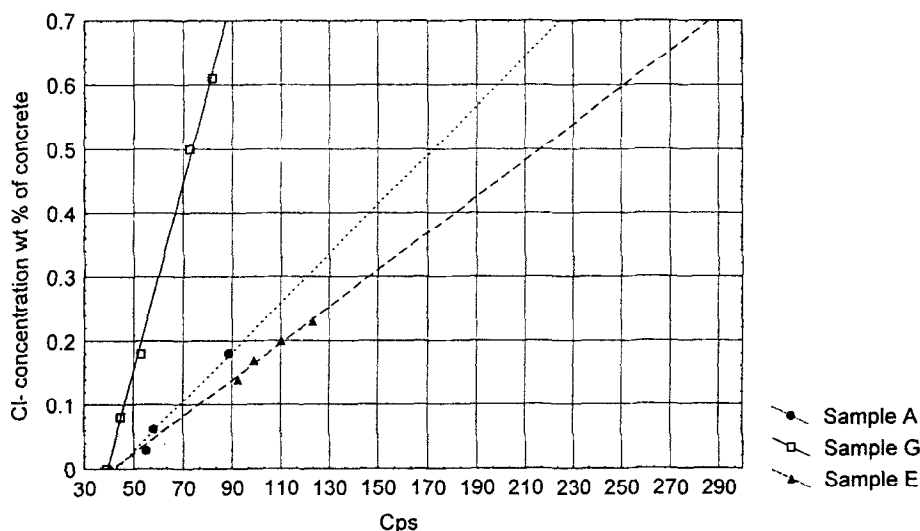


FIG. 2.

Chloride content in concrete evaluated by chemical titration vs. measured Cps at the $\text{Cl K}\alpha_1$ peak.

The results of the second experimentation are summarised in Figure 2. In this case real chloride concentrations (measured by chemical titration measurements) are compared to the mean counts per second (Cps) collected at the $\text{K}\alpha_1$ Cl peak on the same sample during XRF. It is evident that at the same chloride concentration Cps is lower for sample G than samples A and E, a minor difference is evident between samples A and E, interpolating line slopes being 0.015 (wt% Cl/Cps), 0.003 and 0.004 (wt % Cl/Cps) respectively.

Discussion

Looking at the results it is evident that the choice of calibration standard type is of fundamental importance to the accurate determination of chloride content in concrete specimens. Chloride is present in contaminated concrete either in a bonded form as a salt (calcium chloro-aluminate hydrates, e.g. Friedel's salt), as an interlaminar complex chemisorbed by calcium silicate hydrate, and in a soluble form in the pore solution (12, 13, 14). Standard preparation by adding ground NaCl could be the factor which influences XRF measurements. As already mentioned chloride characteristic X ray intensity emitted by the sample depends not only on element concentration but also on powder grain size, degree of compaction and chemical bindings of the element in the matrix (8,10). The effect of grinding was evaluated and clearly shown on measurements performed on samples A. A portion of roughly ground concrete (grain size about 2 mm) was mixed with NaCl salt (grain size about 0.2 mm) to obtain a chloride concentration of 0.5 wt% and the mixture mill ground for different times. XRF measurements evidenced a noticeable decrease of $\text{K}\alpha_1$ Cl peak Cps vs. time (continuous line in Figure 3).

On the other hand by preparing the XRF sample by mechanical mixing of concrete ground for 60 s (mean grain size 5 μm) and NaCl (0.5 wt% chloride concentration) ground for different times a limited Cps reduction was noted (dashed line in Figure 3). However it

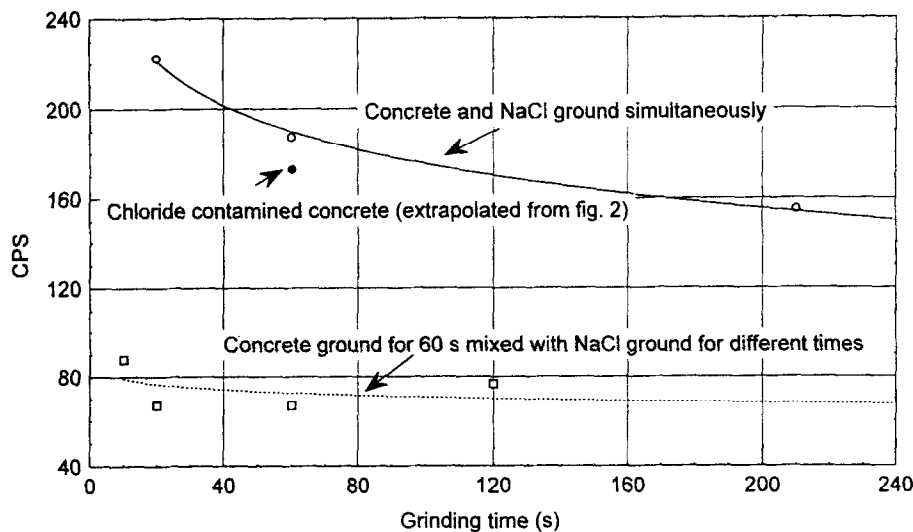


FIG. 3.

Cps at the $K\alpha_1$ Cl peak on A type samples as a function of grinding time for a chloride concentration of 0.5 wt% by concrete.

should be stressed that in this last case NaCl grain size did not reduce greatly with increasing grinding time (Table 4) since grain agglomeration, as observed by Scanning Electron Microscopy, occurred.

Thus the difference between the two cases could be due to an increase of grinding effect for the NaCl when previously mixed to concrete powder.

An extensive investigation on the effect of heterogeneity on XRF analysis has been carried out by Claisse and Samson (15). By idealizing a two phase sample as a bidimensional array of fluorescent regions of length l and non fluorescent regions of length ml (where m is the ratio between volume concentration of the nonfluorescent phase and the volume concentration of the fluorescent phase) they proposed the following equation, for very low concentrations, to evaluate the fluorescent intensity ($I(\lambda_s)$) from a given mixture as a function of the fixed parameter μ''_n and μ''_f and the variable l :

TABLE 4
Influence of Grinding Time on Mean Grain Size of NaCl

Grinding time (s)	Mean grain size (μm) [by laser granulometry]
10	50
20	23
60	29
120	43

$$I(\lambda_s) = \frac{k\mu_E C_E I_0(\lambda_p)}{\mu_f l} \left[1 + \frac{(1 - e^{-\mu_f l})(\mu_f - \mu_n)}{\mu_f \mu_n} \right] \quad (1)$$

where

μ''_f is the sum of the linear absorption coefficient of the fluorescent compound for the primary radiation (excitation radiation) and the linear absorption coefficient for the secondary radiation (the fluorescence radiation);

μ''_n is the sum of linear absorption coefficient of the nonfluorescent compound for the primary radiation and the linear absorption coefficient for the secondary radiation;

$I_0(\lambda_p)$ is the primary radiation beam intensity;

k is the product of the fluorescent yield and the solid angle of emission;

C_E is the global volume concentration of the fluorescent element;

μ_E is the mass absorption coefficient of the fluorescent element for the primary radiation.

TABLE 5

Absorption Coefficients for Selected Elements after Heinrich (16)

Element	Elementary composition (wt %)	Mass absorption coefficient for $\text{Cl K}\alpha_1$ cm^2/g	Mass absorption coefficient for $\text{Rh L}\alpha$ cm^2/g	Mass absorption coefficient for $\text{Rh L}\beta_1$ cm^2/g
	Concrete after Hungerford (17) density=2.3 g/cm^3			
Fe	1.4	816.4	756.1	657.7
H	1.0	-	-	-
O	52.9	303.7	280.5	242.9
Mg	0.2	899.2	831.4	720.9
Ca	4.4	354.4	328.2	285.5
Si	33.7	1367.8	1265.5	1098.4
Na	1.6	690.2	638.2	553.4
K	1.3	299.5	277.4	241.2
Al	3.4	1116.6	1032.7	896.0
C	0.1	111.3	102.7	88.9
	Sodium Chloride density=2.16 g/cm^3			
Na	60.65	690.2	638.2	553.4
Cl	39.35	207.1	191.8	1854.6

TABLE 6
Values of Parameters Used in Equation 1

$\mu_E(\text{cm}^2/\text{g})$	$\mu''_f(\text{cm}^{-1})$	$\mu''_n(\text{cm}^{-1})$	m	$C_E(\text{g}/\text{cm}^3)$	$kI_0(\lambda p)$ (Cps)*
690.46	2281	3054	72.76	0.01776	18865

*calculated from measurements carried out on a 100% NaCl disk

In our case, for simplicity, only the $L\alpha$ and $L\beta_1$ lines of Rh (2.696 and 2.834 KeV their energies, 100 and 42 their relative intensity respectively) can be considered as excitation radiations. By using the mass absorption coefficient table reported by Heinrich (16) (Tables 5, 6) and the elementary composition (wt%) of a Portland concrete after Hungerford (17), for a concrete-NaCl mixture (0.5 wt% by concrete) Equation 1 gives the curve reported in Figure 4.

The effect of grinding is evident though less marked than in actual conditions probably due to simplification related to the model adopted.

However the difference noticed between chloride contaminated concrete and NaCl-concrete mixture is yet to be explained. In the former case chloride is contained in the solution of the capillary pores of concrete ranging from 0.010 to 1 μm . Since porosity could be due either to the hydrated cement paste or to the aggregates and considering that the mean size of the milled concrete powder is about 5 μm it could be possible to suppose that chloride was intimately mixed within the matrix, that is to say that the fluorescence phase and the

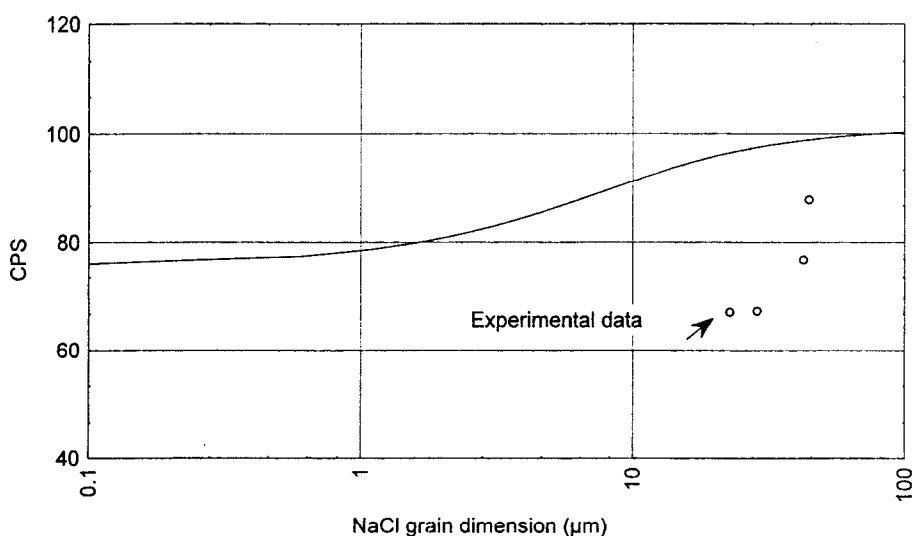


FIG. 4.

Cps vs. grain dimension as calculated by equation 1 for 0.5 wt% by concrete chloride concentration.

nonfluorescence phase are coincident ($\mu''_f = \mu''_n = 3054 \text{ cm}^{-1}$). In this case Equation 1 reduces to

$$I(\lambda_s) = \frac{k\mu_E C_E I_0(\lambda_p)}{\mu_n}$$

which for $m \rightarrow 0$ gives $I(\lambda_s) = 49 \text{ Cps}$, which, also in this case, is much lower than the experimental value. The resolution of the problem could be connected to the influence of the chemical composition of the fluorescent phase. When the concentration of the fluorescent elements are very small (m very large), as in our case, as reported by Claisse, the intensity ratio of the large-grain to fine grain sample is equal to μ''_f/μ''_n . It is concluded that, if $\mu''_f < \mu''_n$, the intensity should decrease when the grain size increases. μ''_n depends on cement type and mainly on aggregate type (especially on its silicon content, having silicon a high absorption coefficient for the $\text{Cl K}\alpha$ line), also μ''_f depends on chemical composition of the chloride containing phase (e.g. sodium chloride, calcium chloro-aluminate hydrates, calcium silicate hydrate complexes). Since absorption coefficients depend greatly on the spectra of the primary radiation too, a theoretical evaluation of resulting value of $I(\lambda_s)$ is quite difficult.

Such considerations are confirmed by measurements carried out on samples A and E (Figure 3). In this case the different chemical composition of the pore solution and different Cl bonding condition could be the cause of their distinct response to XRF measurements.

In a recent work Reefman (18) proposed an analytical and a numerical approach to evaluate the effective absorption coefficient (μ^{eff}) in a multi-phase powder, developing an expression for the total reflected intensity in a heterogeneous powder in terms of concentration and particle size. A characteristic in the calculation is that the distribution function of the grains is similar to the correlation function used in dense fluid mechanics, where particle-particle correlations are important. The calculated μ^{eff} , for average grain diameters (d) comparable to the inverse of the absorption coefficient, differs sensibly from the commonly used formulae for the absorption coefficient (a linear combination of the constituting μ) the μ^{eff}/μ_i ratio ranging, for a two component system (A: non fluorescent phase, B: fluorescent phase), between 0.4 to 4 as a function of the ratio μ_A/μ_B . However referring to our experimental results where the μ''_n/μ''_f ratio is equal to 1.34 and the average absorption coefficient μ is approximately $4 d^{-1}$, the estimated errors in the evaluation of the absorption coefficient are almost negligible and leading furthermore to a reduction of the grain size dependence of $I(\lambda_s)$. After Reefman, great importance could be due also to other parameters such as surface roughness and particle texture which can lead to an estimation error of the evaluation of μ^{eff} of over 20%. Such uncertainty in the measurement are however an order of magnitude lower than the difference evidenced in this work between contaminated chloride concrete and chloride added concrete and could not therefore be indicated as the only factor affecting the measurements.

Conclusions

To determine chloride content in concrete structures X-ray fluorescence is a suitable analytical method to be used when a great number of measurements have to be carried out. However a number of problems could affect the validity of the measurement.

Chloride fluorescence intensity, at the same concentration level and at very low concentrations, is greatly reduced when chloride is present in the concrete matrix as NaCl salt instead of being dissolved in pore solution, due to different absorption coefficient of the two chloride containing phases. In the former condition fluorescence intensity is directly proportional to NaCl mean grain size.

Pore solution composition also seems to influence chloride fluorescence intensity, the latter being higher when chloride is forced to migrate into concrete by an electrical field rather than being allowed to penetrate by diffusion.

To avoid these problems, when performing XRF measurements concrete samples whose chloride content has been evaluated by other analytical techniques (e.g. chemical titration) should be used as calibration standards. However such a limitation reduces the convenience of using XRF analysis to cases where a great number of determinations on similar samples has to be carried out.

References

1. AASHTO T 260 (1984).
2. ASTM C 1202 (1994).
3. UNI 7928 (1978).
4. ACI 201.2R (1977).
5. ACI 318 (1983).
6. K. Pettersson, Corrosion and Corrosion Protection of Steel in Concrete, p.461, Sheffield Academic Press, Sheffield, 1994.
7. W. Lukas e G. Hartl, Zem. Beton, 26, 180 (1981).
8. H. Stanjek e H. Dörner, TIZ, 111, 99 (1987).
9. H. Stanjek e H. Dörner, TIZ, 111, 159 (1987).
10. G.R. Lachance, F. Claisse, Quantitative X-ray Fluorescence Analysis, 224, John Wiley & Sons, Chichester (1995).
11. R. Cigna, G. Familiari, F. Gianetti, E. Proverbio, Corrosion and Corrosion Protection of Steel in Concrete, p.878, Sheffield Academic Press, Sheffield, 1994.
12. Rasheeduzzafar, S.E. Hussain and S.S. Al-Saadoun, Cem. Conc. Res., 21, 777 (1991).
13. C.L. Page and Ø. Vennesland, Matériaux et Constructions, 16, 19 (1983).
14. M.N. Haque and O.A. Kayyali, Cem. Conc. Res., 25, 531 (1995).
15. F. Claisse and C. Samson, Advance in X-ray Analysis Vol. 5, p. 335, Plenum Press, New York, 1962.
16. K.F.J. Heinrich, D.L. Vieth and H. Yakowitz, Advances in X-ray Analysis Vol. 9, p. 208, Plenum Press, Denver, 1966.
17. H.E. Hungerford, Reactor Materials, Vol 1., p.1086, Interscience Publishers, New York, 1960.
18. D. Reefman, Philips Research Materials Analysis, 3, 37 (1996).